Evaluation of Artifact Subspace Reconstruction for Automatic EEG Artifact Removal

Conference Paper *in* Conference proceedings: ... Annual International Conference of the IEEE Engineering in Medicine and Biology Society. IEEE Engineering in Medicine and Biology Society. Conference · June 2018

DOI: 10.1109/EMBC.2018.8512547

4 authors:

Chi-Yuan Chang
University of California, San Diego
2 PUBLICATIONS **6** CITATIONS
SEE PROFILE

Sheng-Hsiou Hsu
University of California, San Diego
21 PUBLICATIONS **97** CITATIONS
SEE PROFILE

Luca Pion-Tonachini
University of California, San Diego
15 PUBLICATIONS **56** CITATIONS
SEE PROFILE

Tzyy-Ping Jung
University of California, San Diego
328 PUBLICATIONS **18,517** CITATIONS
SEE PROFILE

Evaluation of Artifact Subspace Reconstruction for Automatic EEG Artifact Removal

Chi-Yuan Chang, *Student Member, IEEE,* Sheng-Hsiou Hsu, *Student Member, IEEE,* Luca Pion-Tonachini, *Student Member, IEEE,* and Tzyy-Ping Jung, *Fellow, IEEE*

***Abstract*— One of the greatest challenges that hinder the decoding and application of electroencephalography (EEG) is that EEG recordings almost always contain artifacts – non-brain signals. Among existing automatic artifact-removal methods, artifact subspace reconstruction (ASR) is an online and real-time capable, component-based method that can effectively remove transient or large-amplitude artifacts. However, the effectiveness of ASR and the optimal choice of its parameter have not been evaluated and reported, especially on real EEG data. This study systematically validates ASR on ten EEG recordings in a simulated driving experiment. Independent component analysis (ICA) is applied to separate artifacts from brain signals to allow a quantitative assessment of ASR's effectiveness in removing various types of artifacts and preserving brain activities. Empirical results show that the optimal ASR parameter is between 10 and 100, which is small enough to remove activities from artifacts and eye-related components and large enough to retain signals from brain-related components. With the appropriate choice of the parameter, ASR can be a powerful and automatic artifact removal approach for offline data analysis or online real-time EEG applications such as clinical monitoring and brain-computer interfaces.**

I. Introduction

Electroencephalography (EEG) has been widely used in the fields of neuroscience [1], clinical assessment [2], and brain-computer interfaces. One of the greatest challenges that hinders the decoding and application of EEG is that EEG recordings are almost always contaminated by artifacts such as electrode impedance changes caused by headset motion as well as eye-blink, eye-movement, neck and scalp muscle activities. Traditionally, these artifacts were removed manually by visual inspection [3], which could be time-consuming, laborious, subjective, and not feasible in online and real-time applications [4].

To automate the artifact removal process, earlier methods used channel-based statistical-thresholding approaches to remove abnormal activities [5] or adaptive filters with additional reference channels to regress out targeted artifacts [6]. But these methods either could not reconstruct clean data or require auxiliary channels. Another popular approach is to separate artifacts from brain signals using independent component analysis (ICA) [3] and then apply classifiers to identify and reject the artifact-related independent components (ICs) [7]. However, the ICA-based methods were less effective in removing transient, non-biological artifacts such as abrupt impedance changes due to headset motions and were computationally expensive and generally for offline analyses.

To address the challenges, Kothe and Jung [8] proposed the artifact subspace reconstruction (ASR) approach, which is an automatic, online-capable, component-based artifact removal method that could be useful in removing transient or large-amplitude artifacts. ASR is similar to principal component analysis (PCA)-based method in which large-variance components are rejected and channel data are reconstructed from remaining components. The main difference is that ASR automatically identifies and utilizes clean portions of data to determine thresholds for rejecting components. Although recent studies [1] [9] have indicated the potential use of ASR as a powerful data-cleaning method, the effectiveness of ASR and the guidelines for choosing its parameter have never been reported or validated, especially on real EEG data.

This study systematically validates the effectiveness of ASR on ten EEG recordings from ten subjects performing a simulated driving experiment, where artifacts induced by EEG headset motions and activities from eye-blink, eye-movement, and scalp muscle are present. We first characterize the performance of ASR with different cutoff parameters that determine the rejection thresholds. Next, we apply ICA to separate artifacts and brain signals, which allows the quantitative assessment of ASR's effectiveness in removing various types of artifacts and in preserving brain activities. Finally, we report the cross-subject results and provide insights into the optimal choice of ASR's parameter.

II. Materials and Methods

A. Dataset and data preprocessing

To evaluate ASR, we used an EEG dataset collected from 10 subjects performing a sustained attention task in a driving simulator [10]. In the 90-min experiment, the subjects responded to randomly presented lane-departure events by steering the car back to the cruising position as soon as possible. Therefore, we expected the presence of intermittent artifacts in the EEG data such as from electrical interference, EEG headset motions, and activities from neck and scalp muscle, eye-blink, and eye movement. For each subject, 32-channel EEG data were recorded by a NeuroScan System at 500 Hz sampling rate. The electrodes (Ag/AgCl) were placed on the scalp according to the international 10-20 system.

C.-Y. Chang and S.-H. Hsu contribute equally to this work.

This work was supported in part by a gift fund, KreutzKamp TMS RES F- 2467, to TPJ and the Army Research Laboratory through the Cooperative Agreement under Grant W911NF-10-2-0022.

C.-Y. Chang, S.-H. Hsu, and T.-P. Jung are with Dept. of Bioengineering (BIOE) and Swartz Center for Computational Neuroscience (SCCN) of University of California, San Diego (UCSD).

L. Pion-Tonachini is with Dept. of Electrical and Computer Engineering and SCCN of UCSD.

To remove high-frequency noise, the EEG data were cleaned by a band-pass FIR filter (0.5-100 Hz) and then were down-sampled to 250 Hz. Next, we removed channels with mostly negligible activity (flat line threshold: 5), noisy signals (noisy line threshold: 4), or a poor correlation with adjacent channels (correlation threshold: 0.8) using *clean_rawdata*, an EEGLAB plug-in function [11].

B. Artifact Subspace Reconstruction (ASR)

The mathematical derivation and technical details of ASR are available in [8][9]. Here, we briefly describe the three-step ASR process and emphasize some of its key aspects and advantages.

In the first step, ASR automatically selects clean portions of EEG signals based on the distribution of signal variance. Specifically, ASR calculates channel-wise root-mean-square (RMS) values on each 1-second window, z-scores the values for each channel across the windows, identifies clean windows in which the z-scored values are within -3.5 and 5.5, and concatenates the clean windows to obtain calibration data X_C. It is worth noting that the length of selected calibration data may vary depending on the noise level of the data.

In the second step, ASR determines the rejection criteria on the principal-component (PC) space of the calibration data and obtains thresholds based on the distribution of the signal variance on that space. Specifically, ASR computes the covariance matrix of X_C, a square (mixing) matrix M_C where $M_C M_C^T = \text{Cov}(X_C)$, and eigenvalue decomposition of $M_C = V_C D_C V_C^T$ where V_C and D_C contain eigenvectors and eigenvalues respectively. Once the data are projected onto the component space $Y_C = V_C^T \cdot X_C$, ASR calculates the mean μ_i and standard deviation σ_i of RMS values across all 0.5-second windows of Y_C for each component i, and then defines rejection thresholds as $T_i = \mu_i + k \cdot \sigma_i$ where k is a user-defined (cutoff) parameter.

In the third and final step, ASR applies an eigenvalue decomposition to the covariance matrix of EEG segments $\text{Cov}(X) = VDV^T$ along a sliding window with window size of 0.5 seconds and a step size of 0.25 seconds. In each window, ASR identifies the PCs (eigenvector, V_j) with variance (eigenvalue, D_j) larger than the rejection thresholds T_i projected from V_C onto V: $D_j > \sum_i (T_i V_{Ci}^T V_j)^2$. Finally, ASR reconstructs the clean window data using the equation:

$$X_{clean} = M_C \cdot (V_{trunc}^T M_C)^\dagger \cdot V^T \cdot X$$

where V_{trunc}^T refers to truncated eigenvectors retaining only un-rejected PCs. It is important to note that ASR is not simply rejecting PCs but rejecting projected PCs defined by $V^T M_C$.

The Matlab scripts for performing ASR are available as an open-source plug-in function *clean_rawdata*() in EEGLAB [11]. While many parameters can be optimized, the most important user-defined parameter is the cutoff parameter k for determining the rejection thresholds. This study aims to characterize the effectiveness of ASR in removing artifacts and how k affects its performance.

C. Evaluating performance of ASR using ICA

We apply ICA to evaluate the effectiveness of ASR for removing artifact while preserving brain signals. ICA assumes EEG data x can be modeled as a linear mixture A of statistically independent sources s ($x = As$) and learns an unmixing matrix W such that the independent components (ICs) recover the original sources $y = Wx \approx s$. ICA has been widely used for separating stereotyped brain processes and various types of artifacts such as muscle, eye-blink, and lateral eye-movement activities [3]. In this study, we employ extended Infomax ICA [12], which is available in the *runica* function in EEGLAB.

Based on the ICA decompositions of ASR-cleaned data, we can quantitatively assess the extent to which ASR affects the activities of the brain and artifactual ICs in the following two ways. Firstly, we compute the component-wise correlation coefficients of the best-matched ICs between ICA decompositions of EEG data with and without ASR cleaning, i.e. $\text{Corr}(A^{(k)}, A^{(\infty)})$ where k refers to ASR's cutoff parameter and $k = \infty$ refers to no ASR correction, using the Hungarian method in the *matcorr* function in EEGLAB. This enables the examination of whether artifact ICs are removed and whether brain ICs are retained. Secondly, we select stereotyped ICs from $A^{(\infty)}$, apply the corresponding spatial filters $W^{(\infty)} = (A^{(\infty)})^\dagger$ to ASR-cleaned data $X^{(k)}$, calculate the IC activations $Y^{(k)} = W^{(\infty)} X^{(k)}$, and compare the power reduction for each IC (i.e., $\text{Var}(Y_i^{(k)}) - \text{Var}(Y_i^{(\infty)})$). This allows us to examine the effectiveness of ASR for reducing the activities of artifactual ICs and preserving that of brain ICs.

III. Results and Discussion

A. Overall effects of ASR cleaning

Fig. 1 shows the percentage of data points modified by ASR (i.e. rejecting at least one component) and the average of the variance reduction of the data before and after ASR cleaning using different cutoff parameters k from a sample subject. As expected, ASR modified more data points and removed more signal variance when lower k was applied. When $k = 100$, less than 3% of data was modified, yet it accounted for more than 10% of variance reduction. This indicates abnormal, large-amplitude artifacts were removed, which were unlikely to be brain signals. When $k = 10$–20, the two curves crossed over between 60% to 75% which matched the percentage of non-calibration data (61%). When $k = 5$–7, as previously suggested in [9], nearly 90% of data was modified and up to 80% of the variance was reduced, implying both artifacts and brain signals could be removed and the thresholds might be too aggressive.

B. Changes in ICA decompositions

To evaluate what types of signals were removed by ASR, Fig. 2(A) plots the changes, in terms of component-wise correlation coefficients, in ICA decompositions of the EEG data from the same subject as a function of cutoff parameters k. Fig 2(B) shows the corresponding IC scalp maps, i.e. the

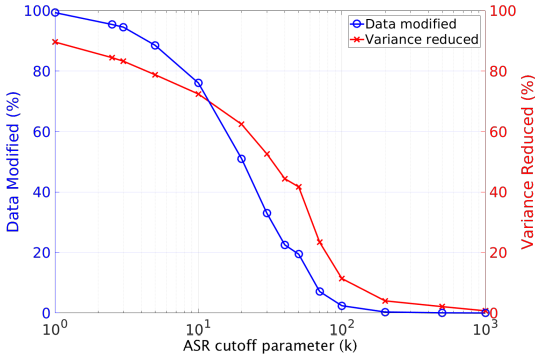

Fig. 1: The percentage of data modification (blue) and variance reduction (red) by ASR with different cutoff parameters for a sample subject.

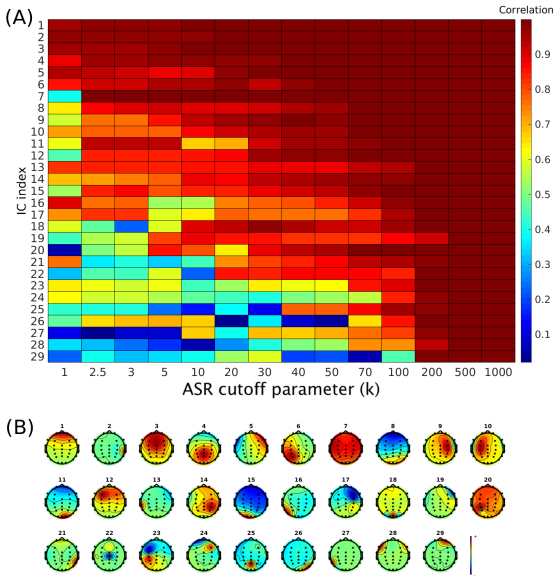

Fig. 2: (A) Component-wise correlation coefficients of the best-matched ICs between ICA decomposition of the EEG data without ASR cleaning (template ICs) and those with ASR cleaning using different ASR cutoff parameters. The IC index is sorted by the coefficients average across cutoff parameters. (B) The scalp maps of the template ICs.

spatial distribution of each source activities over the scalp channels, of the ICA decomposition of the EEG data without ASR cleaning, which serves as the template to be compared with.

When ICs in Fig. 2(A) were sorted in decreasing order by average correlations, we found that those top ICs, which survived the rigorous cleaning of ASR with a small k, were likely to be associated with brain activities (IC3, 4, 6 and 8). These ICs were characterized by spatially homogeneous scalp maps [13]. On the contrary, those ICs which disappeared when the k was smaller than 70 to 100 were likely to account for artifacts due to single-channel noises (IC22, 27, and 29) or localized muscle activities (IC23), characterized by isolated or sporadic scalp maps. Interestingly, the ICs accounting for eye-blink (IC1) and eye-movement (IC5) activities were also consistently present when different k's were used, indicating that ASR could not completely remove eye-related activities. As a variance-based artifact removal method, ASR might be limited in removing artifact beyond the point where the power of the artifact is comparable to that of brain signals.

C. Changes in IC activities

To further quantify how different types of signals were removed by ASR, we manually selected some of the stereotyped ICs in Fig. 2B that corresponded to the brain, eye and other likely-artifact activities and computed their source activities retained after ASR cleaning with different cutoff parameters as described in Section II-C. Fig. 3(A) shows the results and Fig. 3(B) plots the percentage of the retained power of the selected ICs after ASR. As shown in Fig. 3(A), the power of the eye-related ICs (green) was 5 to 15 times larger than that of the brain-related ICs (blue) in the raw data, but ASR started to reduce the eye activities when the cutoff parameter k was smaller than 100. When k reached 10, more than 90% of the power was removed (Fig. 3(B)), with the retaining power comparable to that of the brain-related ICs. Hence, even though the eye ICs were still found in Fig. 2, the power of the eye activities have been significantly reduced after ASR cleaning.

As for the other likely-artifact ICs (red), their average power was up to 10 times smaller than that of the brain-related ICs in the raw data, mainly because those artifacts were sporadic events. Fig. 3(B) shows that when $k = 100$ the power of likely-artifact ICs could be reduced down to 5% to 25% of original values while the activities of brain-related ICs (blue) remained nearly intact. It is worth noting that IC2 is an exception and further investigation is required.

Although ASR with a lower k value could remove more eye and artifact activities, the power of brain-related ICs (blue) could also be affected. Fig. 3(B) shows that when $k < 100$, the power of the selected brain ICs started to decrease. When $k = 5$–7, as previously suggested in [9], those brain ICs retained only 40% to 80% of their original power. Nevertheless, the brain ICs still preserved larger portions of activities compared with the eye and the other ICs.

In summary, ASR with $k = 10$–100 is recommended, where the artifact-like ICs and their activities could be effectively removed. Within this range, it is the trade-off between removing eye-related activities and retaining brain-related signals. Although only the result of a single subject was reported due to page-limit, these results of other subjects were comparable.

D. Cross-subject analysis

Fig. 4 plots the cross-subject results shown in Fig. 1 for the ten subjects. We found that the overall effects of ASR cleaning, in terms of the portion of data repaired and the percentage of variance reduced, were similar to the sample subject's results (Fig. 1). For example, ASR with $k = 100$ could effectively remove abnormal large-amplitude artifacts,

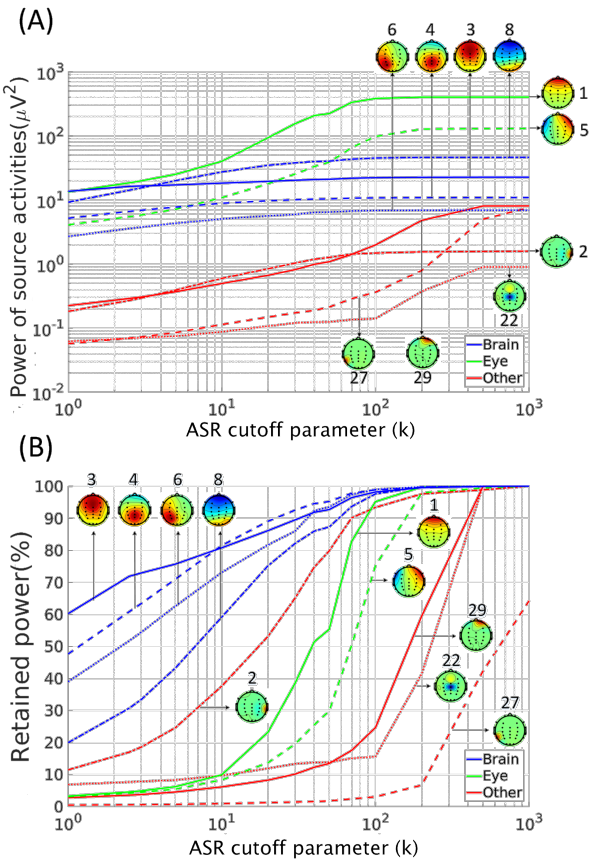

Fig. 3: (A) The power of source activities of selected ICs in Fig. 2 when different ASR cutoff parameters were applied. These ICs were manually classified into the brain (blue), eye (green), and others (red). The scalp maps and indexes of those ICs are also shown. (B) The percentage of retained power of source activities of the same selected ICs.

and ASR with $k = 5$–7 might be too aggressive in removing 70% of the signal variance. However, the two curves crossed at $k = 7$ in Fig. 4 instead of $k = 10$–20 in Fig. 1. This indicates that inter-session variability existed, possibly due to differences in the level of artifact contaminations and the portion selected as calibration data.

IV. Conclusions

This study demonstrates that ASR is an effective automatic artifact removal approach, quantifies its effectiveness in removing different types of signals using ICA, and provides insights into the optimal choice of its parameter. Applied to 10 EEG sessions from 10 subjects in a simulated driving experiment, ASR with a mild threshold ($k = 100$) could effectively remove large-amplitude artifacts, yet ASR with the previously suggested threshold ($k = 5$–7) was too aggressive. Examining the ICA decompositions and activities of ASR-cleaned EEG data from one sample subject, we found that the optimal ASR cutoff parameter might be between 10 to 100, which is small enough to remove activities from artifact and eye-related ICs and large enough to retain signals from brain-related ICs. With the appropriate choice of the parameter, ASR can be a powerful artifact removal approach and can be applied to automatic data cleaning for offline data analysis or online real-time EEG applications such as clinical monitoring and brain-computer interfaces.

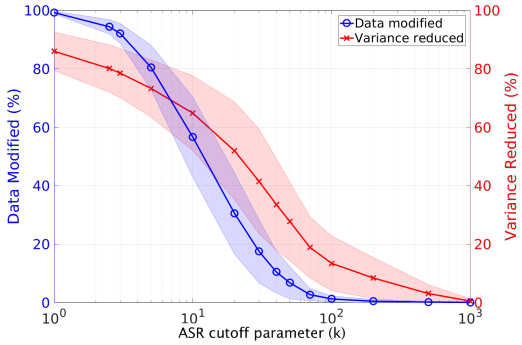

Fig. 4: The percentage of data modification (blue) and variance reduction (red) by ASR with different cutoff parameters average across 10 subjects. The shaded area shows the standard deviation across subjects.

References

[1] F. Artoni, C. Fanciullacci, F. Bertolucci, A. Panarese, S. Makeig, S. Micera, and C. Chisari, "Unidirectional brain to muscle connectivity reveals motor cortex control of leg muscles during stereotyped walking," *NeuroImage*, vol. 159, pp. 403–416, 2017.

[2] A. Steiger, U. von Bardeleben, T. Herth, and F. Holsboer, "Sleep eeg and nocturnal secretion of cortisol and growth hormone in male patients with endogenous depression before treatment and after recovery," *J. of Affective Disorders*, vol. 16, no. 2-3, pp. 189–195, 1989.

[3] T.-P. Jung, S. Makeig, C. Humphries, T.-W. Lee, M. J. McKeown, V. Iragui, and T. J. Sejnowski, "Removing electroencephalographic artifacts by blind source separation," *Psychophysiology*, vol. 37, no. 2, p. 163178, 2000.

[4] Urigüen, J. Antonio, and B. Garcia-Zapirain, "Eeg artifact removalstate-of-the-art and guidelines," *J. of Neural Eng.*, vol. 12, no. 3, 2015.

[5] M. Jas, D. Engemann, Y. Bekhti, F. Raimondo, and A. Gramfort, "Autoreject: Automated artifact rejection for meg and eeg data," *NeuroImage*, vol. 159, pp. 417–429, 2017.

[6] A. Schlögl, C. Keinrath, D. Zimmermann, R. Scherer, R. Leeb, and G. Pfurtscheller, "A fully automated correction method of eog artifacts in eeg recordings," *Clin. Neurophysiol.*, vol. 118, pp. 98–104, 2007.

[7] Y. Zou, V. Nathan, and R. Jafari, "Automatic identification of artifact-related independent components for artifact removal in eeg recordings," *IEEE J. of Biomed. and Health Inform.*, vol. 20, no. 1, 2016.

[8] C. A. E. Kothe and T.-P. Jung, "Artifact removal techniques with signal reconstruction," *U.S. Patent Application No. 14/895,440*, 2014.

[9] T. R. Mullen, C. A. Kothe, M. Chi, A. Ojeda, T. Kerth, S. Makeig, T.-P. Jung, and G. Cauwenberghs, "Real-time neuroimaging and cognitive monitoring using wearable dry eeg," *IEEE Trans. on Biomed. Eng.*, vol. 62, pp. 2553–2567, 2015.

[10] R.-S. Huang, T.-P. Jung, and S. Makeig, "Tonic changes in eeg power spectra during simulated driving," *Foundations of Augmented Cognition. Neuroergonomics and Operational Neuroscience*, vol. 5638, pp. 394–403, 2009.

[11] A. Delorme and S. Makeig, "Eeglab: an open source toolbox for analysis of single-trial eeg dynamics including independent component analysis," *J. of neurosci. methods*, vol. 134(1), pp. 9–12, 2004.

[12] T.-W. Lee, M. Girolami, and T. J. Sejnowski, "Independent component analysis using an extended infomax algorithm for mixed subgaussian and supergaussian sources," *Neural Comput.*, vol. 11, no. 2, pp. 417–441, 1999.

[13] A. Delorme, J. Palmer, J. Onton, R. Oostenveld, and S. Makeig, "Independent eeg sources are dipolar," *PLoS ONE*, vol. 7, 2012.